

Article

# Arc Shape Characteristics with Ultra-High-Frequency Pulsed Arc Welding

Mingxuan Yang <sup>\*</sup>, Hao Zheng and Ling Li

Department of Materials Processing, Beijing University of Aeronautics and Astronautics, Beijing 100191, China; sy1507203@buaa.edu.cn (H.Z.); Liling2016@buaa.edu.cn (L.L.)

\* Correspondence: yangmingxuan@buaa.edu.cn; Tel.: +86-138-1189-1251

Academic Editor: Hai-Lung Tsai

Received: 17 October 2016; Accepted: 7 December 2016; Published: 3 January 2017

**Abstract:** Arc plasma possesses a constriction phenomenon with a pulsed current. The constriction is created by the Lorentz force, the radial electromagnetic force during arc welding, which determines the energy distribution of the arc plasma. Welding experiments were carried out with ultra-high-frequency pulsed arc welding (UHFP-AW). Ultra-high-speed camera observations were produced for arc surveillance. Hue-saturation-intensity (HSI) image analysis was used to distinguish the regions of the arc plasma that represented the heat energy distribution. The measurement of arc regions indicated that, with an ultra-high-frequency pulsed arc, the constriction was not only within the decreased arc geometry, but also within the constricted arc core region. This can be checked by the ratio of the core region to the total area. The arc core region expanded significantly at 40 kHz at 60 A. A current level of 80 A caused a decrease in the total region of the arc. Meanwhile, the ratio of the core region to the total increased. It can be concluded that arc constriction depends on the increased area of the core region with the pulsed current (>20 kHz).

**Keywords:** arc constriction; ratio of core region to the total; pulsed arc welding

---

## 1. Introduction

Arc welding is a traditional process technology in industry. It has been developed through a long history of studying its mechanism and engineering applications. However, many phenomena lack a systematic approach, which includes the arc constriction. With classical theory, it was found that the parallel current lines attracted each other when they were in the same direction. This is also applicable in an arc plasma [1] with direct current welding (DC welding). Most of the time, DC arc welding creates the current pointing from the base metal to the electrode. The current is formed during the movements of electrons and positive particles. The current elements with the same direction can be recognized as the current line series. They will attract each other with a macro perspective as one is surrounded in the electromagnetic field created by another. Mutual attraction occurs between any two lines or elements. It can be deduced that the Lorentz force, which is the major electromagnetic force and only changes the direction of charged particles, would constrict the arc plasma in a radial direction, which is called arc constriction. This phenomenon has been proved by experiments [2]. Arc constriction will create a pinched arc plasma [3] during the welding process. It is regularly believed to increase the stiffness, arc voltage, and energy density of the arc plasma. As a result, it will enhance the penetration and reduce the shielding area of the welding arc, which is important for the arc welding process. Firstly, constriction of the arc leads to an increased arc temperature and axial flow velocity with the increased current density [4]. Significant results can usually be obtained under the condition of a large welding current greater than 150 A [5,6] and a pulsed current [7,8]. The research [9] revealed an increased arc voltage with different shielding gases, which displayed obvious arc constriction. Secondly, some results indicate significant constriction with the pulsed welding process [10,11]. Previous work indicates

that the root radius decreased during pulsed arc welding [12], and the attenuation coefficient of the magnetic force is defined to evaluate the intensity of the arc constriction, even though it was a direct reflection of the constriction view. Thirdly, some studies demonstrated the effect of arc constriction on the weld appearance [13,14], which was also proved with pulsed welding [15]. Previous work found an increase in the arc voltage and arc constriction with pulsed welding [16]. Such reflections could be correlated with the arc constriction during pulsed arc welding. Finally, the continued arc shapes were displayed to exhibit the arc constriction with an ultra-high-speed camera most of the time. Some experiments found the increased arc size with a large current [17,18], although that caused the arc constriction. Thus, the arc constriction is predicted to have other reflections with a pulsed arc plasma of more than 20 kHz. Furthermore, visual observation is very popular in arc plasma surveillance; it can be used to track characteristic elements and to conduct arc plasma diagnosis by imaging of the continuous spectra [19]. At the same time, it is simple and rapid to analyze the distribution of the temperature field using the method of image processing, and the dynamic change of the arc plasma can be monitored in real time by a high-speed camera, and the image processing methods are required in order to distinguish the region of the arc plasma for further study.

Above all, the welding arc core region and the edge of the arc contain plenty of information about the welding arc physics, and it is meaningful to study the ratio of the arc core region to the total region. This paper studies the principle of arc constriction in order to experiment, conjecture, and verify. The aim is to contribute to arc diagnosis with respect to the pulsed arc constriction.

## 2. Methods

Figure 1 shows the diagrammatic drawing of a visual inspection system for the gas tungsten arc welding (GTAW); snapshot (a) is the simplified model of (b). The system contains two parts: Part 1, which is included by red rectangle, is the welding system, consisting of a welding source, tungsten welding electrode, shielding gas, weldment, and workspace. It is used for providing the experiment with a stable welding arc plasma. Conventional and pulsed current of 60 and 80 A are both used in the experiment, with argon as the shielding gas and Ti-6Al-4V titanium alloy as weldment. Part 2, which is included by blue rectangle, reveals the visual measuring system, which consists of high-speed camera and computer. Dimmer filter ND4, which is in front of the high-speed camera lens, is used for decreasing the arc brightness. The high-speed camera collects the real-time image processing signal of the welding process and transmits the signal to the computer via USB. The computer is able to control the time of exposure, sampling time, and some other parameters of the high-speed camera and save the video signal. Average pulsed current of 60 A has a peak current of 80 A and a base current of 40 A, average pulsed current of 80 A has a peak current of 110 A and a base current of 50 A, and the peak duration is all 50%. Finally, conventional and pulsed frequencies of 20 and 40 kHz, both under currents of 60 and 80 A, are used in the GTAW, and the video information is obtained.

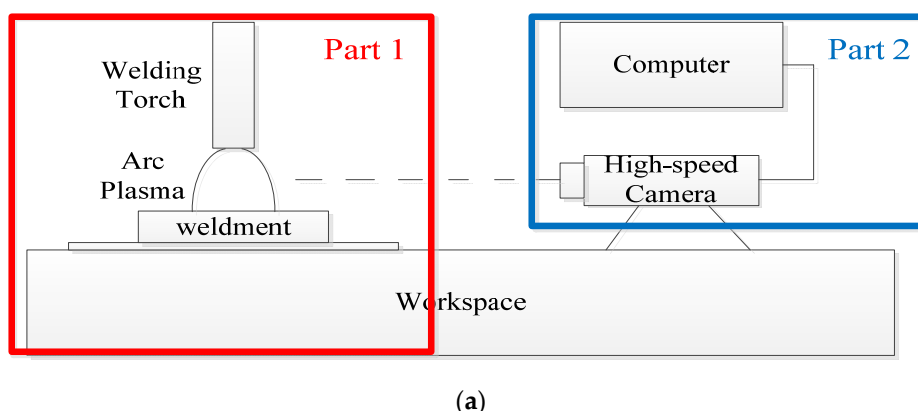


**Figure 1. Cont.**

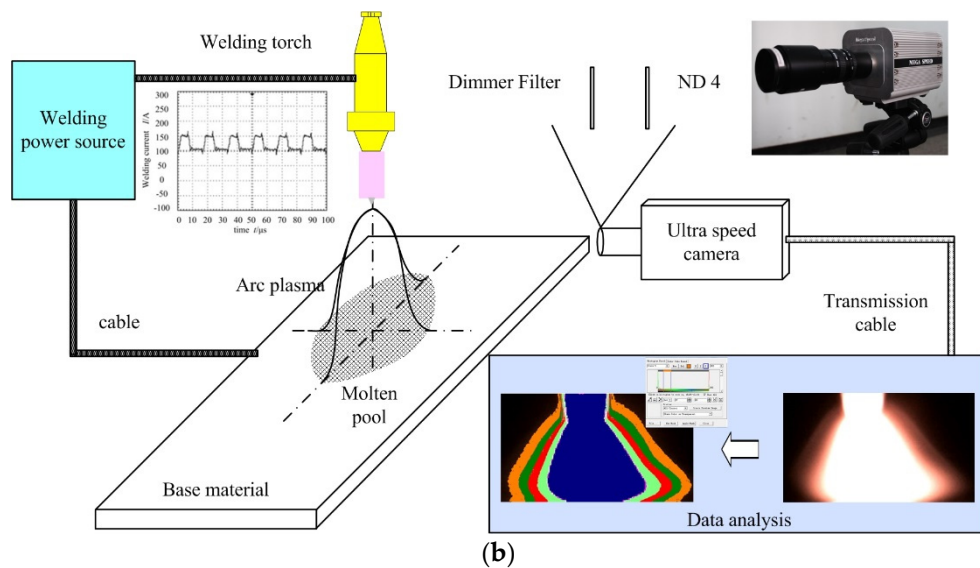


**Figure 1.** Visual inspection system for gas tungsten arc welding (GTAW): (a) simplified model; (b) physical model.

In the process of obtaining the GTAW images using the high-speed camera, there are always some noise signals, including natural lighting, the influence of arc welding voltage and current, and so on, affecting the brightness of arc. The final result will be affected by noise signals. In this paper, MATLAB, manufactured by American corporation MathWorks (Natick, MA, USA), is used for image de-noising by using the method of median filtering [20], which is a nonlinear signal processing technology to suppress the isolated noise, effectively based on order statistical theory. The feature of median filtering is, at first, to establish a square neighborhood, which is centered on any point. Then, the filter takes every point in the neighborhood, also called the filtering window, in order, substituting the median value for the original one. The image could be subject to a smoothing process when the window moves. The median filtering method has simple arithmetic, low time complexity, and self-adaptive simplification. Based on this, the paper uses the method of median filtering to suppress the noise using a  $3 \times 3$  filtering window. Based on MATLAB, the images will be processed in two steps as follows:

1. Make a welding arc regionalization for de-noised images, the core region is located near the medial axis of the welding arc plasma, where the arc has the highest temperature, most concentrated plasma, largest current density, most drastic ionization thermal motion, and highest energy. It is also a prime source of energy for the melt of the base material. The shape, voltage, and force, or some other parameters of welding arc, vary with the welding arc core region.

2. Calculating the ratio of the welding arc core region with respect to the total. The ratio represents the energy transfer efficiency from the welding cathode to the base material. Plenty of scholars have tried to improve the energy transfer efficiency and a number of papers have been published about it. As a result, it is rather valuable to research and discuss matters about the ratio of the core region to the total.

### 3. Results and Discussion

With the descriptions in Section 2, the arc regions were distinguished. The edges of the images, as one of the fundamental image features, contain plenty of image information, as they contain the irregular structure, unstable phenomenon, and the abruptly changeable signal points [21]. These points show the outline of the figure and give some very important characteristic conditions while conducting image edge detection. The signal points of abrupt change are regarded as the points of the edge, and the change of the gray value could be reflected by the contiguous gray value gradient distribution. However, the method of image processing remains a macro-view cognition to diagnose the arc's

physical properties because the arc shape, shown by the high-speed camera, is not able to display the scope of every part inside the arc. Meanwhile, ionization zones vary with the shooting conditions. As a result, it is quite difficult to determine the edge of the arc with the method of image processing. Spectrum analysis is an efficient way to recognize the edge of the arc. According to Xiao [22], it is possible to obtain the curves of variation in light intensity from the core region to the edge of the arc by using spectroscopic methods [23]. As a result, the ratio of the trough to the peak of the curve can be obtained, which represents the edge of the arc to the core of the arc. An approximation method is used, simultaneously, to obtain the ratio of the welding arc core region to the total region. Calculating the two ratios above, the gray value of the edge of the arc is about 15. It is well known that the range from 95%–100% of the energy is the power core, which is relevant to the welding arc intensity of light. Therefore, 95% of the highest gray value defines the edge of arc core region, 15, as the edge of the arc total region.

### 3.1. De-Noising Processing

Figure 2 displays the original drawing, grey-scale map, median filtering once, and median filtering twice, respectively. The gray-scale value histogram is illustrated on the right side of Figure 2. The horizontal axis represents the gray-scale values, and the vertical axis represents the corresponding quantity of the gray-scale values of the grey-scale map, median filtering once, and median filtering twice, respectively. The results indicated the variation tendency of the de-noised image and its gray-scale value quantity was not obvious, and it can be found that there were few noise signals while collecting the visual signals with the high-speed camera. Taking gray-scale value 4 into account as an example, the grey-scale map, median filter once and twice had 17,855 points, 17,978 points, and 18,024 points. Thus, the difference demonstrated that the de-noising processing worked to remove a small number of noises, although the visual signal collected was of rather high quality. Above all, it can be concluded that the regularity is similar under the different welding currents and pulse frequencies using the same disposal method.

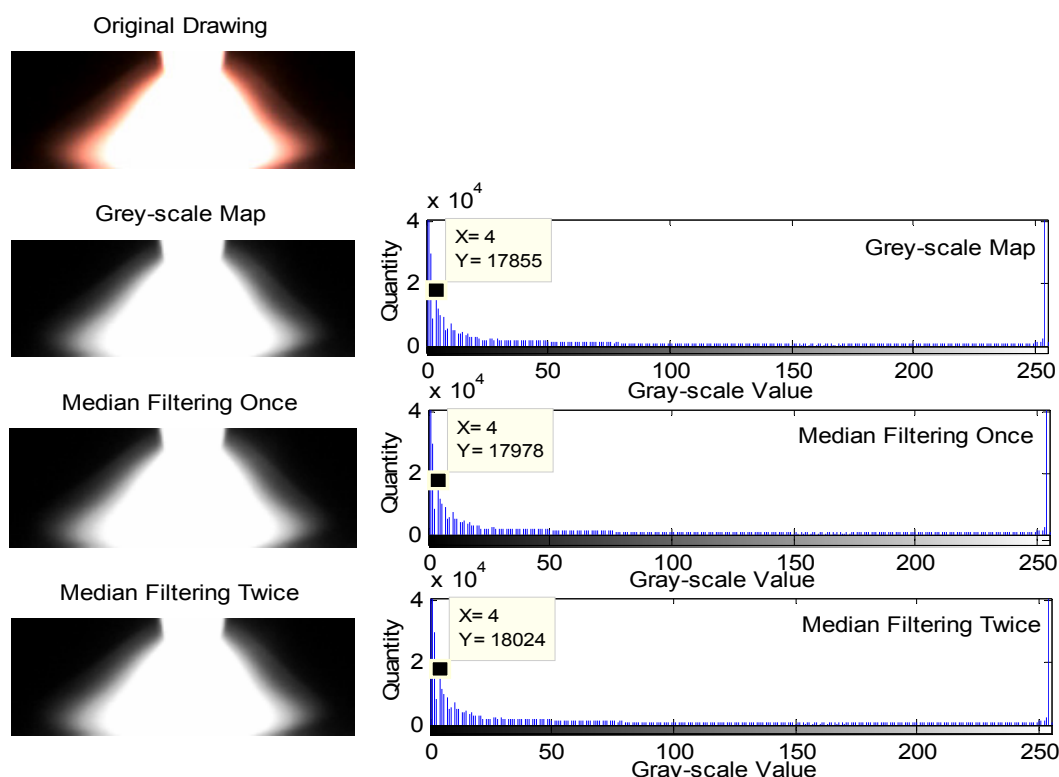


**Figure 2.** De-noising processing (80 A, 20 kHz).

### 3.2. Arc Regionalization

Arc regionalization is an important part of the study of the welding mechanism [24]. This paper considers the selection of the region edges as the key point, and the analysis is produced with the core region and the edge of the welding arc. With the image processing mentioned before, Figure 3 illustrates a consequence of regionalization at 80 A and at 20 kHz. Compared with the original one, the critical gray-scale values of every area edge are 242.25, 167, 91, and 15 from the center to the outside. The gray-scale value 15 is proved as a boundary according to the curves of variation in intensity from the center to the outer edge. Note that the crimson part is the arc core region with the highest temperature in which the arc possessed the most concentrated plasma, the largest current density, the most drastic ionization thermal motion, and the largest energy. The other area of the arc is occupied by the other zones. Figure 4 illustrates a front view of the arc and a top-down view sliced in the maximal radius of the arc. The ratio of the core region to the total area is 59.92%. The method above is capable of examining the ratio of the core region to the total area, and it is simpler and more convenient.

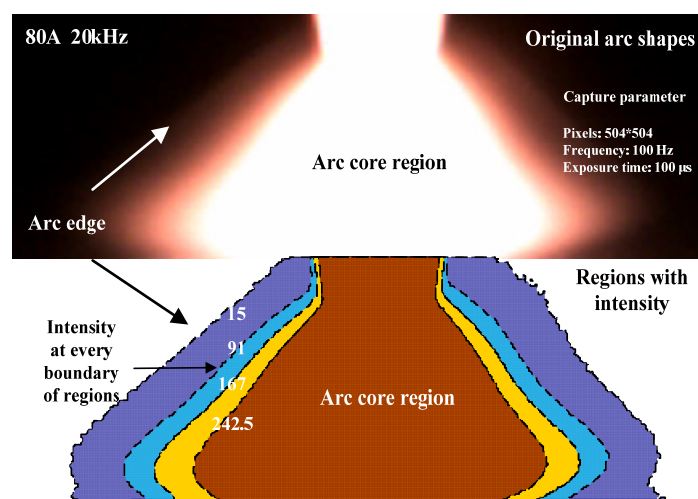


**Figure 3.** Arc regionalization.

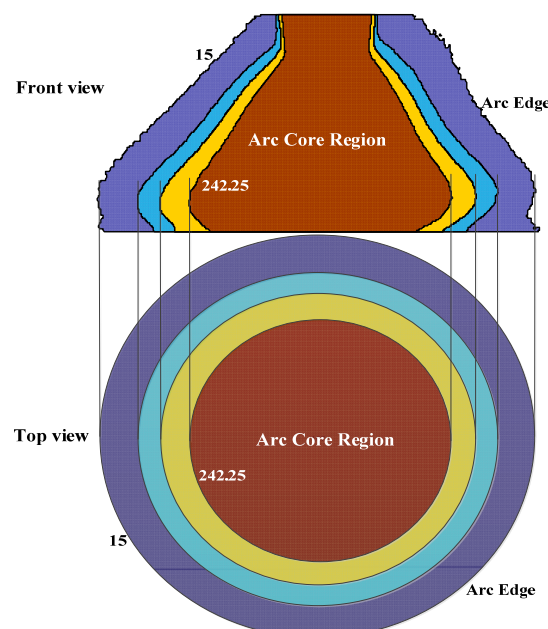


**Figure 4.** Front view of the arc and top-down view sliced in the maximal radius of the arc.

### 3.3. Arc Core Region, Total Area and the Ratio of the Core Region to the Total Area

Under the circumstance of different currents and pulsed frequencies, images that contain stable welding arc physical information are chosen when the welding tungsten electrode is fully burning and the welding arc is burning persistently. Based on MATLAB, we get the area relative value by counting the amount of pixel points. The core region area, the total area, and the ratio of the core region to the total area are calculated, and the average values of the data obtained are presented in Table 1.

**Table 1.** Average data of the core region area relative value, the total area relative value, and the ratio of the core region to the total area. C-DC means conventional direct current.

Frequency \ Current	60 A			80 A		
	Core Area	Total Area	Core/Total	Core Area	Total Area	Core/Total
40 kHz	236,662	462,110.5	0.51213	270,029.5	501,016	0.53896
20 kHz	233,596.5	462,005.5	0.50562	257,142.5	497,471.5	0.51691
C-DC	202,868	426,122	0.47609	246,720.5	488,955	0.50458

Figure 5 illustrates the core and total areas against the pulsed frequencies. It is a double-coordinate line chart, with the horizontal axis representing the pulsed frequency and 0 kHz representing the conventional direct current, while the vertical axis on the left shows the region area relative value with 60 A and, on the right, it indicates the region area relative value with 80 A. The total arc region expanded with the large current, which coincided with the classical theory. That means the arc with the large energy input possessed a larger portion of the region. A possible reason for this is that more ionization results in a greater particle collision region. The welding current can be maintained in an expanded region as the charged particles are enough to guarantee the stable current transformation. Thus, the welding current level from 60 to 80 A made a large total area of the arc plasma. The current increased by 33% and, in contrast, the total arc region increased by 14.75%. Furthermore, the core region expanded with the large total area, and the increasing rate was about 22%. The ratio of the core region to the total increased from 47.7% to 50.5%.

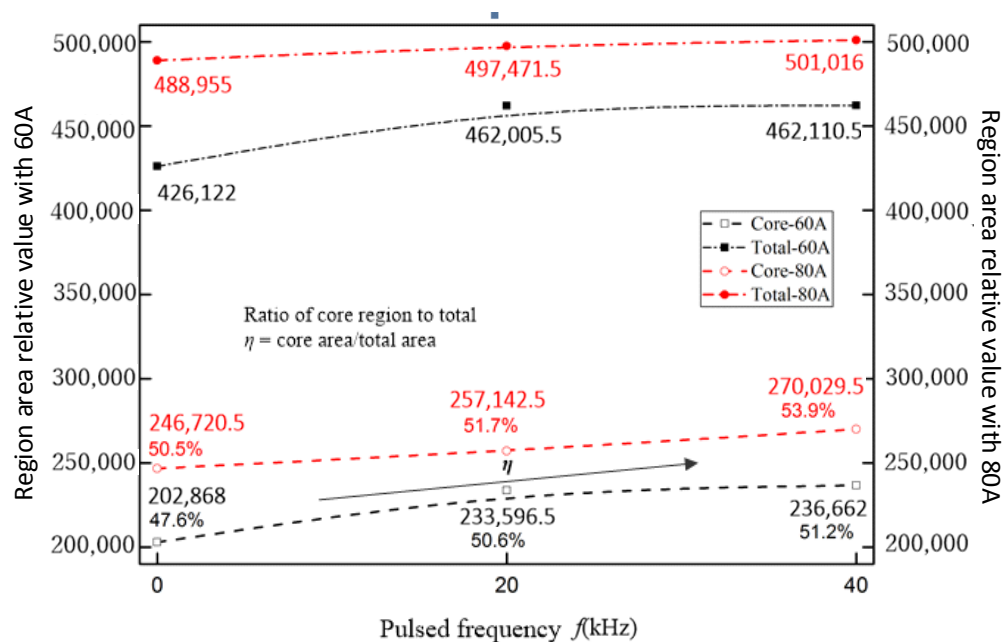


**Figure 5.** Core region and the total area.

When the current is constant at 60 or 80 A, from conventional DC to a pulsed frequency of 20 or 40 kHz, a larger core region, total area, and ratio of the core region to the total area can be found. At the 60 A current level, the absolute values were larger in the core/total regions with the increasing pulse frequency. The effect of the pulsed current was significant with the expanded core region, which increased by 15%, at least compared with C-GTAW (Conventional-GTAW). Furthermore, the ratio of the core region to the total area was even more than C-GTAW at the 80 A level. It needs to be noted that the differences of the absolute areas between 20 and 40 kHz were not significant. However, the ratio was 51.2% at 40 kHz, which meant a large core region. The variation of the arc total area shows the shrinkage-expansion of the arc shape. The variation of the core region reflects not only the ionization thermal motion, temperature, and current density, but also the shape, force, and others; it is a sign of the transmission of energy. As for the ratio of the core region to the total area, it is the efficiency of the energy transfer from the cathode to the arc to the welding material [25]. Obviously large currents can create more energy input with larger arc plasma. The ratio of the core region was recognized as the result of the energy concentration or arc constriction. The classical theory indicated the radial electromagnetic force compressed the arc plasma with a large or pulsed current. The results above demonstrated the increased arc region at 20–40 kHz; however, the core region was larger than C-GTAW. That meant a large ratio of the core region in arc plasma. We can also assume the movement of dynamically charged particles. The particles with large kinetic energy will be affected by a large Lorentz force, and they will be forced to deflect to the center of the arc plasma, which would create a region with a large absolute energy density. Additionally, the region can be assumed to possess a large current density. Significant numbers of moving particles can be predicted in this region and light, and transferred energy reflections with collisions or other processes will be much easier to capture, and they are displayed in Section 3.2. The authors predict that the energy input to the base metal is mostly from the core region.

It can be concluded that when the pulsed current frequency is constant at 20 kHz, 40 kHz, or C-GTAW, with a current of 80 or 60 A, the arc plasma possesses a constriction phenomenon both for the total area and the core region, a lower ratio of the core region to the total area, a lower temperature, a smaller current density, a slower ionization thermal motion, and a lower efficiency of energy transfer. When the current is constant at 60 or 80 A, from a pulsed frequency of 40 kHz to 20 kHz to C-GTAW, the arc plasma possesses the same phenomenon. Above all, the effect of the pulsed arc plasma can be considered as the constriction, which reflects an expanded core region. The large ratio of the core region means there is energy concentration, or the enlarged area of the high energy region. This phenomenon is created by the Lorentz force which deflects the charged particles, especially for electrons that have large velocities. Such a deflection causes more possibilities for collisions which would create more heat or higher temperatures. Thus, the heat input of the arc plasma is believed to be more effective with a pulsed current, and the pulsed arc is supposed to obtain significant penetration.

#### 4. Conclusions

Arc plasma possesses a constriction phenomenon, which is created by the Lorentz force that deflects the charged particles and causes more collisions, for the total area and the core region, a lower ratio of the core region to the total area, a lower temperature, a smaller current density, a slower ionization thermal motion, and a lower efficiency of energy transfer. Heat input of the arc plasma is more effective with a pulsed current. Comparing the current of 80 and 60 A, 60 A responds more obviously when switching C-GTAW to a pulsed current. Eighty ampere responds more obviously to switching to the pulsed frequency of 20–40 kHz.

**Acknowledgments:** This work is supported by the National Natural Science Foundation of China under grant No. 51405007, No. 51675031 and the Fundamental Research Funds for the Central Universities of China. All support from Beijing University of Aeronautics and Astronautics is highly appreciated.

**Author Contributions:** Mingxuan Yang and Ling Li conceived and designed the experiments; Mingxuan Yang and Ling Li performed the experiments; Mingxuan Yang and Hao Zheng analyzed the data; Hao Zheng contributed analysis tools; Mingxuan Yang and Hao Zheng wrote the paper.

**Conflicts of Interest:** The authors declare no conflict of interest.

## References

1. Xu, G.; Hu, J.; Tsai, H.L. Modeling 3D Plasma Arc in Gas Tungsten Arc Welding. *ASME J. Manuf. Sci. Eng.* **2012**, *134*, 031001. [[CrossRef](#)]
2. Palani, P.K.; Murugan, N. Selection of parameters of pulsed current gas metal arc welding. *J. Mater. Process. Technol.* **2006**, *172*, 1–10. [[CrossRef](#)]
3. Yang, X.; Hu, J.; Pallis, J. Simulation of Gas Tungsten Arc Welding Arc in COMSOL. In Proceedings of the ASME-IMECE, Houston, TX, USA, 9–15 November 2012.
4. Murphy, A.B.; Tanaka, M.; Yamamoto, K.; Tashiro, S.; Sato, T.; Lowke, J.J. Modelling of thermal plasmas for arc welding: The role of the shielding gas properties and of metal vapour. *J. Phys. D Appl. Phys.* **2009**, *42*, 194006. [[CrossRef](#)]
5. Fujii, H.; Sumi, Y.; Tanaka, M. Effect of gravity on arc shape in GTA welding. *J. Mater. Sci. Technol.* **2003**, *19*, 209–211.
6. Zhang, S.S.; Cao, M.Q.; Wu, D.T.; Zou, Z.D. Effects of process parameters on arc shape and penetration in twin-wire indirect arc welding. *Front. Mater. Sci. China* **2009**, *3*, 212–217. [[CrossRef](#)]
7. Cook, G.E.; El-deam, H.; Eassa, E.H. The effect of high frequency pulsing of a welding arc. *IEEE Trans. Ind. Appl.* **1985**, *21*, 1294–1299. [[CrossRef](#)]
8. Zhao, J.R.; Sun, D.; Hu, S.S. Arc behavior of high frequency pulse TIG welding arc. *Trans. China Weld. Inst.* **1992**, *13*, 59–66.
9. Murphy, A.B. The effect of metal vapour in arc welding. *J. Phys. D Appl. Phys.* **2010**, *43*, 434001. [[CrossRef](#)]
10. Jin, O.; Yoshisa, A.; Masayasu, N.; Mitsuo, K.; Onuma, A.; Funamoto, T. Development of a new high-frequency, high-peak current power source for high constricted arc formation. *Jpn. J. Appl. Phys.* **2002**, *41*, 5821–5826.
11. Ghosh, P.K.; Dorn, L.; Hübner, M.; Goyal, V.K. Arc characteristics and behavior of metal transfer in pulsed current GMA welding of aluminum alloy. *J. Mater. Process. Technol.* **2007**, *209*, 163–175. [[CrossRef](#)]
12. Yang, M.X.; Qi, B.J.; Cong, B.Q.; Liu, F.J.; Yang, Z.; Chu, P.K. Study on electromagnetic force of arc plasma with by ultrahigh frequency pulsed GTAW of Ti-6Al-4V. *IEEE Trans. Plasma Sci.* **2013**, *41*, 2561–2568. [[CrossRef](#)]
13. Li, M.Q.; Wang, X.H.; Zou, Z.D.; Wu, J. Effect of activating flux on arc shape and arc voltage in tungsten inert gas welding. *Trans. Nonferr. Met. Soc. China* **2007**, *17*, 486–490. [[CrossRef](#)]
14. Howse, D.S.; Lucas, W. Investigation into arc constriction by active fluxes for tungsten inert gas welding. *Sci. Technol. Weld. Join.* **2000**, *5*, 189–193. [[CrossRef](#)]
15. Balasubramanian, M.; Jayabalan, V.; Balasubramanian, V. Effect of process parameters of pulsed current tungsten inert gas welding on weld pool geometry of titanium welds. *Acta Metall. Sin.* **2010**, *23*, 312–320.
16. Qi, B.J.; Yang, M.X.; Cong, B.Q.; Liu, F.J. The effect of arc behavior on weld geometry by high frequency pulse GTAW process with 0Cr18Ni9Ti stainless steel. *Int. J. Adv. Manuf. Technol.* **2013**, *66*, 1545–1553. [[CrossRef](#)]
17. Hu, J.; Tsai, H.L. Effects of Welding Current on Droplet Generation and Arc Plasma in Gas Metal Arc Welding. *J. Appl. Phys.* **2006**, *100*, 053304. [[CrossRef](#)]
18. Pierce, S.W.; Burgardt, P.; Olson, D.L. Thermocapillary and arc phenomena in stainless steel welding. *Weld. J.* **1999**, *78*, 45s–52s.
19. Zong, R.; Chen, J.; Wu, C.; Padhy, G.K. Influence of shielding gas on undercutting formation in gas metal arc welding. *J. Mater. Process. Technol.* **2016**, *234*, 169–176. [[CrossRef](#)]
20. Faragallah, O.S.; Ibrahem, H.M. Adaptive switching weighted median filter framework for suppressing salt-and-pepper noise. *Int. J. Electron. Commun.* **2016**, *70*, 1034–1040. [[CrossRef](#)]
21. Hasan, S.M.A.; Ko, K. Depth edge detection by image-based smoothing and morphological operations. *J. Comput. Des. Eng.* **2016**, *3*, 191–197.
22. Xiao, T. A Study on Conductive Mechanism of TIG Welding Arc and Its Energy Distribution. Ph.D. Thesis, Beijing University of Technology, Beijing, China, 8 June 2013.

23. Xiao, X.; Xueming, H.; Yixiong, W. Comparison of temperature and composition measurement by spectroscopic methods for argon–helium arc plasma. *Opt. Laser Technol.* **2015**, *66*, 138–145. [[CrossRef](#)]
24. Zhenbo, Z.; Jianchao, G.; Jinlong, L.; Liangxian, C.; Ruihua, Z.; Xiongbo, Y.; Junjun, W.; Lifu, H.; Chengming, L. Effect of area arc distribution on diamond nucleation. *J. Synth. Cryst.* **2014**, *43*, 2515–2521.
25. Wei, Y.; Hua, Z.; Zhigang, J.; Hon, K.K.B. Multi-objective optimization of arc welding parameters: The trade-offs between energy and thermal efficiency. *J. Clean. Prod.* **2016**, in press. [[CrossRef](#)]



© 2017 by the authors; licensee MDPI, Basel, Switzerland. This article is an open access article distributed under the terms and conditions of the Creative Commons Attribution (CC-BY) license (<http://creativecommons.org/licenses/by/4.0/>).